Passivity-Based Control Improvement of Single-Link Flexible Manipulators by a Two-Degree-of-Freedom PID Motor Controller

Andrés San-Millán Rodríguez(a) ⋆ and Emiliano Pereira González(b)

(a)Escuela Técnica Superior de Ingenieros Industriales, Universidad de Castilla-La Mancha, Av. Camilo José Cela, s/n 13071, Ciudad Real, España
(b) Escuela Politécnica Superior, Universidad de Alcalá, Ctra.Madrid-Barcelona, Km. 33,600, 28805 Alcalá de Henares, Madrid, España

Abstract. A new approach to a previous passivity-based control scheme of single-link flexible manipulators is presented herein. Such previous scheme achieves precise positioning of the link tip by combining a position angular control of the motor (inner loop) with a link vibration damping (outer loop), which can be designed independently by decoupling joint and link dynamics with a linear strain feedback. Although, precise positioning can be achieved under large tip payload changes, the used inner loop cannot eliminate the steady-state position error due to the nonlinearities present in the motor. The contribution presented in this work consists of using a two-degree of freedom PID motor controller to solve this problem, eliminating thus the steady-state error while also improving the settling time of the angular position. Simulation and experimental results are carried out to illustrate these improvements.

1 Introducción

"Flexible robots" or "flexible manipulators" exhibit many advantages over their rigid counterparts such as they are lighter robots which can be driven using smaller amounts of energy, being more suitable for aerospace industry. In addition, these robots are safer to operate due to their reduced inertia and their inherent property to transform kinetic energy into potential energy (i.e., link strain). However, the vibrations make accurate positioning or trajectory tracking a challenging task, motivating a huge research in this topic [1].

In order to address control objectives, such as tip-position accuracy or suppression of residual vibration, many techniques derived from the control theory have been applied to flexible robots. Most of these control techniques can be classified in two groups: adaptive control [2–4], and robust control [5–7]. Both

⋆ This paper was sponsored by the Spanish FPU Program (Ministerio de Educación, Cultura y Deporte). This paper was sponsored by the Spanish Government Research Program with the Project DPI2012-37062-CO2-01 (Ministerio de Economia y Competitividad) and by the European Social Fund.

robust control and adaptive control usually require complex design methodologies and may show unstability issues due to high frequency unmodeled dynamics of the system due to spillover effects.

Control designs based on the partial differential equations can solve the aforementioned stability problems, while also simplifying the control design. Some examples are the direct strain feedback control (DSFB) [8], and the passivity-based control [9]. However, these techniques present some limitations owing to the coupling between the dynamics of the motor and the link of the flexible manipulator, which may lead to slow time response and position error.

The previous work [10] proposes a passivity-based control scheme consisting of two nested loops which are designed independently by decoupling joint and link dynamics with a linear strain feedback. This scheme damps the vibrations of the tip which appear after the movement of the robot, being also robust to large changes in the payload and to spillover effects. However, the loop used to control the motor angular position cannot remove the steady-state error due to the frictions present in the reduction gear and the motor.

In the present work, this loop is substituted by a two-degree of freedom (2DOF) PID motor controller. Thus, the steady-state error is eliminated while also improving the settling time of the angular position. In addition, a step by step design methodology is proposed to keep the design simplicity of [10]. A design example is simulated and implemented in practice to illustrate these improvements.

2 Dynamic modelling

The scheme of the flexible robot to be controlled is shown in Fig. 1. The system is divided in two subsystems: the subsystem comprising the motor and the gear box, and the subsystem comprising the flexible link with a payload of mass M_p and inertia J_P. The equations of dynamic equilibrium in the joint are:

$$\Gamma_m(t) = n_r K_m V = J_0 \ddot{\theta}_m(t) + \nu \dot{\theta}_m(t) + \Gamma_f(t) + \Gamma_{coup}(t), \tag{1}$$

where Γ_m is the applied torque by the motor, K_m is a constant relating the control voltage of the motor V with the torque in the motor side, J_0 is the hub inertia, n_r is the reduction ratio, θ_m is the angular position of the motor, ν is the viscous friction coefficient, Γ_f is the torque owing to Coulomb friction and Γ_{coup} is the coupling torque between the link and the joint.

The dynamic behavior of an Euler-Bernoulli beam is governed by the following PDE (see, for example [11]),

$$EIw^{IV}(x,t) + \rho w(\ddot{x},t) + c\dot{w}(x,t) = f(x,t). \tag{2}$$

where L is the length of the link, ρ is the volumetric density, EI is the stiffness, w is the deflection, $f(x,t)$ is a distributed external force, c is a damping constant and overdots and primes indicate time and spatial derivatives, respectively.

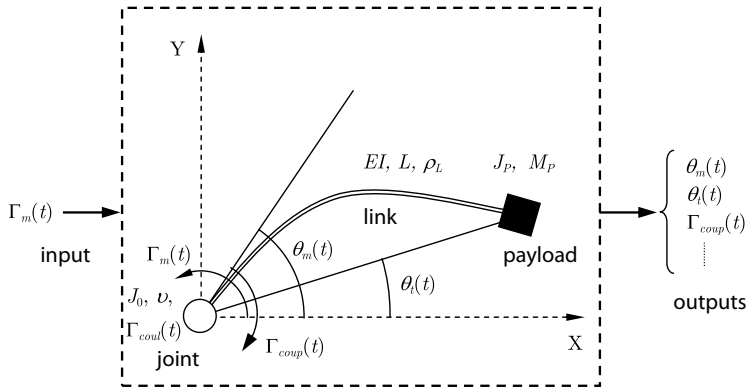

Fig. 1. Robotic system scheme

Solving this equation (see [12]) the transfer functions of the system can be obtained. The assumptions made are that movement of the link is constrained to the horizontal plane (so the gravity effects are negligible), and that the deflections of the link are much smaller than the axial deformation.

The relationship between the coupling torque and the strain measured at the base of the link, which is used to decouple the link from the motor+reduction Gear, is as follows:

$$\Gamma_{coup}(t) = -EIw_0^{''}, \tag{3}$$

where $w_0^{''}$ is the strain at the base of the flexible link.

The model dynamics is derived by considering the link as an Euler-Bernoulli beam (see [12]). In addition, the experimental platform built in the laboratory of the E.T.S.I.I. in Ciudad Real, whose identified system parameters are shown in Table 1, is used to derive the dynamics model needed in the design of the controllers.

Table 1. Experimental platform parameters

Stiffness (Nm^2)	EI	2.4
Thickness (m)	h	0.002
Width (m)	b	0.05
Length (m)	L	1.26
Mass density (Kg/m^3)	ρ	2680
Inertia of the rotor and hub (Kg/m^2)	J_0	0.79
Motor constant (Nm/V)	K_m	0.474
Reduction gear ratio	n_r	50
Viscous friction coefficient (Kgm^2/s)	ν	3.65
Torque owing Coulomb friction (Nm)	Γ_f	17.06

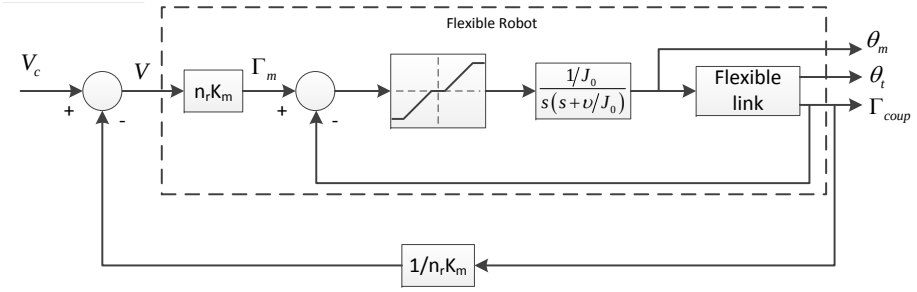

Fig. 2. Decoupling the flexible link and the motor+reduction gear dynamics compensating the coupling torque

3 Control design methodology

The objective of this section is to present the control design methodology based on the passivity property existing between the integral of the coupling torque Γ_{coup} (output) and the motor angle θ_m demonstrated in [10]. The control strategy consists of three sequential steps: First the link and motor dynamics are decoupled, then the controller of the angular position is designed, and finally an outer control loop is designed in order to damp the vibrations of the tip of the link.

The contribution presented in this work consists of substituting the PD motor controller of the inner loop, which was proposed in the design methodology presented in [10], by a 2DOF PID. The tuning of this 2DOF PID motor controller is based on a minimization process, which consists of minimizing the error between the output of the system and a step shaped reference control signal. Once the 2DOF PID is thus correctly tuned, the steady state error is removed and the settling time of the motor angular position is minimised, thus improving the results obtained in [10] without a significant increase of the complexity of design.

3.1 Decoupling the link and the motor dynamics

In order to decouple the link and the motor dynamics is necessary to compensate the coupling torque as showed in Fig. 2. Compensating the coupling torque leads from the original model of the plant to the equivalent one showed in Fig. 3. The coupling torque is obtained in this work by using a strain-gauge bridge placed at the base of the beam (see Eq. (3)). The strain signal is amplified by the dynamic strain amplifier (Kyowa DPM600) and filtered by a second-order Butterworth filter with its cutoff frequency set to 300 Hz.

3.2 Design of the inner loop controller robust to nonlinearities

After decoupling the motor and link dynamics, the modified motor position control scheme is shown in Fig. 4. Note that the whole model of the motor,

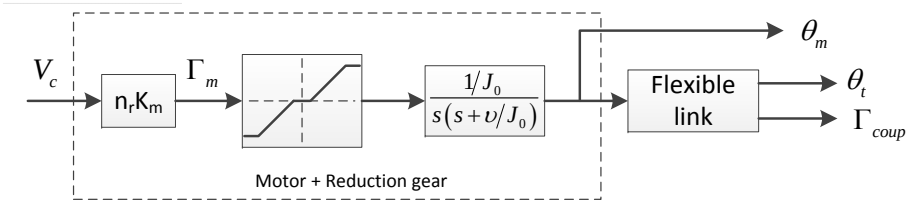

Fig. 3. Equivalent decoupled system

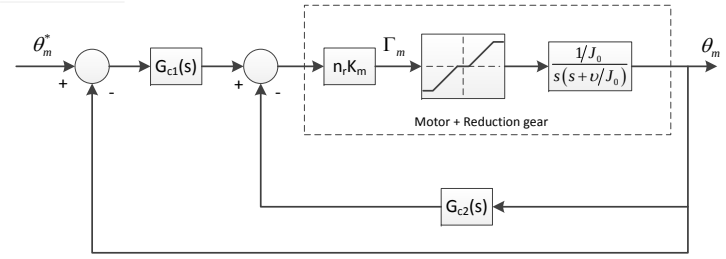

Fig. 4. 2DOF PID applied to the motor+reduction gear model

including the nonlinearities caused by the friction and the saturation of the motor, is considered in order to design the 2DOF PID controller [13].

The relative order of the inner loop dynamics must be less or equal than two in order to guarantee the stability and the passivity properties of the overall control system [10]. Considering this restriction, the 2DOF PID controller design can be divided into the following steps: i) choose the transfer functions $G_{c1}(s)$ and $G_{c2}(s)$ so that the closed loop dynamics (considering only the linear part the motor+reduction gear dynamics) has a relative degree less or equal than two, ii) establish restrictions in the parameters of $G_{c1}(s)$ y $G_{c2}(s)$ in order to simplify the resulting transfer function so that such transfer function has real and coincident zeroes and poles, leading to a second order critically damped system, and iii) adjust the zeroes and poles of the resulting closed loop system in order to minimize the following functional:

$$J(p_1, p_2) = \int_0^\infty (u(t) - y(t))^2 \, t dt, \tag{4}$$

where y(t) is the response of the controlled system (considering the nonlinearities of the motor and the reduction gear), and $u(t)$ is a step reference signal of amplitude equal to 0.5 radians.

If the linear part is only considered in Fig. 4, the transfer function between θ_m and θ_m^* is as follows:

$$G_{BC}(s) = \frac{G_{c1}(s)A}{s^2 + sB + A(G_{c1}(s) + G_{c2}(s))} \tag{5}$$

where A and B are equal to $n_r K_m/J_o$ and ν/J_0, respectively. If it is imposed $G_{BC}(s)$ to being a critically damped second order system, the following functions $G_{c1}(s)$ and $G_{c2}(s)$ can guarantee this restriction:

$$G_{c1}(s) = \frac{a_2 s^2 + a_1 s + a_0}{s^2 + gs}, \;\; G_{c2}(s) = \frac{b_2 s^2 + b_1 s + b_0}{s^2 + gs}. \tag{6}$$

Thus, substituting the equalities (6) into (5) the following expression is obtained:

$$G_{BC}(s) = \frac{A(a_2 s^2 + a_1 s + a_0)}{s^4 + (g+B)s^3 + (Bg + A(b_2 + a_2))\, s^2 + A(b_1 + a_1)s + A(b_0 + a_0)}. \tag{7}$$

Therefore, if it is considered that the transfer function (7) has the following form:

$$G_{BC}(s) = \frac{p_2^2 (s + p_1)^2}{(s + p_1)^2 (s + p_2)^2}, \tag{8}$$

the equations for designing the parameters of (6) from the values of p_1 and p_2 are the following:

$$\begin{aligned}
a_2 &= \frac{p_2^2}{A}, \quad a_1 = \frac{2p_2^2 p_1}{A}, \quad a_0 = \frac{p_2^2 p_1^2}{A} \\
b_2 &= \frac{B(B - 2p_2 - 2p_1)}{A} + \frac{p_2^2 + p_1^2 + 4p_2 p_1}{A} - \frac{p_2^2}{A} \\
b_1 &= \frac{2p_2^2 p_1 + 2p_1^2 p_2}{A} - \frac{2p_2^2 p_1}{A} \\
b_0 &= 0, \quad g = -B + 2p_2 + 2p_1.
\end{aligned} \tag{9}$$

Note that Eq. (8) is an approximation because the Coulomb friction is not considered. This approximation can be used for a range of values for p_1 and p_2. Thus, the optimal values of p_1 and p_2 are obtained by simulation the control scheme of Fig. 4 when the overshot is less than 10%. Fig. 5 shows the evaluation of Eq. (4) after considering the above restrictions, where a minimum value of J can be seen.

3.3 Design of the outer loop

The whole control scheme is shown in Fig. 6, where the inner loop is approximated by the following transfer function:

$$G_{BC}(s) \simeq \frac{p_2^2}{(s + p_2)^2} \tag{10}$$

Note that the nonlinearities of the motor and the coupling between dynamics have been compensated in the previous design steps. This approximation was validated via experimental results with different reference inputs. Thus, if the approximation (10) is considered adequate and if the outer control is defined as follows:

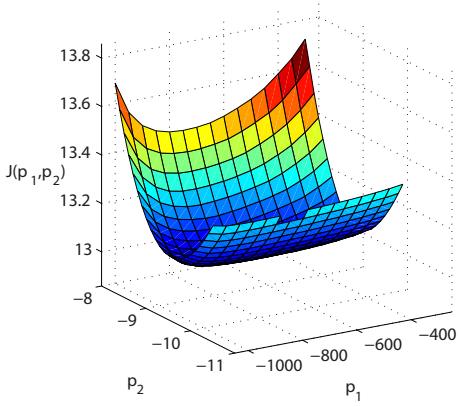

Fig. 5. Evolution of (4) with respect p_1 and p_2

$$C(s) = (1/s)C'(s) = (1/s)K_c(s + \lambda), \tag{11}$$

the passivity property existing between the integral of the coupling torque (measures with the strain gauges) and the angular position of the motor (measured in the encoder of the motor) can be considered to deduce the following necessary and sufficient condition to guarantee the stability of the overall control system(see [10] for more details):

$$Re\left\{\frac{K_c p_2^2(j\omega + \lambda)}{(j\omega + p_2)^2}\right\} > 0, \forall\omega > 0, \tag{12}$$

which can be summarized in:

$$\lambda < 2p_2 \tag{13}$$

Bearing in mind this restriction on the value of λ , the remaining parameter of $C'(s)$ (K_c) is chosen so that the complex conjugate poles corresponding to the first mode of vibration of the link become into a double pole placed in the real axis (critically damped dynamic for the closed loop system).

Note that Eq. (13) is a simple condition of inequality (the same as for the one showed in [10]). However, if a PID is used for the inner control loop instead the 2DOF PID proposed herein, this stability condition is more complex because $G_{BC}(s)$ cannot be approximated by a critically damped second order system.

4 Experimental results and simulations

The identification of the joint dynamics is firstly carried out. This dynamics is as follows:

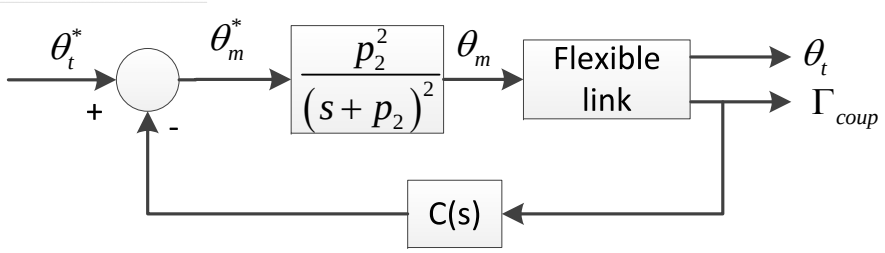

Fig. 6. General control scheme

$$\frac{\theta_m}{V_c} = \frac{39.26}{s(s+4.24)} \tag{14}$$

Based on this model, the functional (4) is minimized to obtain the parameters of Eqs. (6), which determine the optimal regulator for the angular position control. The parameters obtained after the minimisation are shown in the Table 2.

Table 2. Optimal values for the 2DOF PID control

Parameter	Value	Parameter	Value
a_2	2.06	b_2	12218
a_1	2801.7	b_1	$2.1 \cdot 10^5$
a_0	$9.5 \cdot 10^5$	b_0	0
g	1371.8		

Next the transfer function of the flexible link is identified from the experimental platform defined in Table 1:

$$\frac{\Gamma_{coup}}{\theta_m} = s^2 \left(\frac{5}{s^2+0.075s+43.419} + \frac{3.5}{s^2+0.131s+1720.2} + \frac{3}{s^2+0.417s+13439} + \frac{3}{s^2+0.821s+52020} \right) \tag{15}$$

Once the system dynamics are known and the inner loop is designed, the values of λ and K_c can be obtained. Thus, the outer controller, which places the poles of the first vibration mode of (15) into a double pole placed in the real axis and guarantees the condition defined into Eq. (13), is tuned as follows:

$$C(s) = \frac{0.84(s+4.76)}{s} \tag{16}$$

The results obtained applying a step input of amplitude equal to 0.5 radians to the controlled system are shown in Figs. 7(a) and 7(b). It can be seen

that the steady state error of the system is null and the residual vibration is approximately zero after 2s.

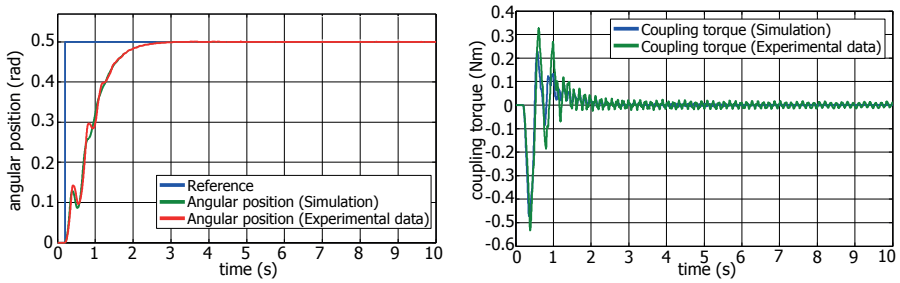

(a) Evolution of the angular position (b) Evolution of the coupling torque

Fig. 7. Step input response (Simulation and experimental results)

Finally, a small oscillation can be appreciated in Fig. 7(b). This oscillation, which corresponds to a high vibration mode, is not significant to obtain a precise tip positioning. It should be remarked that the passivity property (13) does not consider the dynamics of the strain-gauge bridge, the signal amplifier and the low pass filter. These dynamics, which could make the system unstable [14], will be considered in future works.

5 Conclusions

This work has proposed a modification of a previous passivity based control scheme for single link flexible manipulators. This modification is based on substituting the PD motor controller proposed in [10] by a 2DOF PID motor controller. In addition, this modification has been taken into account in a step by step design methodology, which simplifies the controller tuning parameters. The resulting control scheme has been simulated and implemented in a laboratory structure, showing its effectiveness to remove the steady state error position and the residual vibration.

References

1. V. Feliu. Robots flexibles: Hacia una generación de robots con nuevas prestaciones. *Revista Iberoamericana de Automática e Informática Industrial.*
2. T.C. Yang, J.C.S. Yang, and P. Kudva. Load-adaptive control of a single-link flexible manipulator. *Systems, Man and Cybernetics, IEEE Transactions on*, 22(1):85 –91, jan/feb 1992.
3. J.J. Feliu, V. Feliu, and C. Cerrada. Load adaptive control of single-link flexible arms based on a new modeling technique. *Robotics and Automation, IEEE Transactions on*, 15(5):793 –804, oct 1999.

4. A.G. Dharne and S. Jayasuriya. Robust adaptive control of residual vibration in point-to-point motion of flexible bodies. *Journal of Vibration and Control*, 13(7):951–968, 2007.
5. Y.P. Chen and H.T. Hsu. Regulation and vibration control of an fem-based single-link flexible arm using sliding-mode theory. *Journal of Vibration and Control*, 7(5):741–752, 2001.
6. M. Amiri, M.B. Menhaj, and M.J. Yazdanpanh. A neural-network-based controller for a single-link flexible manipulator: Comparison of ffnn and drnn controllers. In *Neural Networks, 2008. IJCNN 2008. (IEEE World Congress on Computational Intelligence). IEEE International Joint Conference on*, pages 1686 –1691, june 2008.
7. V.G. Moudgal, W.A. Kwong, K.M. Passino, and S. Yurkovich. Fuzzy learning control for a flexible-link robot. *Fuzzy Systems, IEEE Transactions on*, 3(2):199 –210, may 1995.
8. Z.H. Luo. Direct strain feedback control of flexible robot arms: new theoretical and experimental results. *Automatic Control, IEEE Transactions on*, 38(11):1610 –1622, nov 1993.
9. Liang-Yih Liu and King Yuan. Noncollocated passivity-based pd control of a single-link flexible manipulator. *Robotica*, 21(2):117–135, March 2003.
10. E. Pereira, I.M. Diaz, J.J.L. Cela, and V. Feliu. A new design methodology for passivity-based control of single- link flexible manipulators. In *Advanced intelligent mechatronics, 2007 IEEE/ASME international conference on*, pages 1 –6, sept. 2007.
11. L. Meirovitch. *Principles and Techniques of Vibrations*. Prentice Hall International, 1997.
12. F. Bellezza, L. Lanari, and G. Ulivi. Exact modeling of the flexible slewing link. In *Robotics and Automation, 1990. Proceedings., 1990 IEEE International Conference on*, pages 734–739 vol.1, 1990.
13. K. Ogata. *Ingeniería de control moderna 4ED*. Pearson educación. Pearson-Prentice-Hall, 2003.
14. J.R. Forbes and C.J. Damaren. Single-link flexible manipulator control accommodating passivity violations: Theory and experiments. *IEEE Transactions on Technology*, 20(3):652–262, 2012.